J|A|C|S
ARTICLES
Published on Web 04/04/2003

Quantitative Analysis and Characterization of DNA Immobilized on Gold

Dmitri Y. Petrovykh,*,†,‡ Hiromi Kimura-Suda,§ Lloyd J. Whitman,‡ and Michael J. Tarlov§

Contribution from the Physics Department, University of Maryland, College Park, Maryland 20742, Naval Research Laboratory, Washington, DC 20375, and National Institute of Standards and Technology, Gaithersburg, Maryland 20899

Received November 22, 2002; E-mail: dmitri.petrovykh@nrl.navy.mil

Abstract: We describe the complementary use of X-ray photoelectron spectroscopy (XPS) and Fourier transform infrared (FTIR) spectroscopy to quantitatively characterize the immobilization of thiolated $(dT)_{25}$ single-stranded DNA (ssDNA) on gold. When electron attenuation effects are accurately accounted for in the XPS analysis, the relative coverage values obtained by the two methods are in excellent agreement, and the absolute coverage can be calculated on the basis of the XPS data. The evolution of chemically specific spectral signatures during immobilization indicates that at lower coverages much of the DNA lies flat on the surface, with a substantial fraction of the thymine bases chemisorbed. At higher immobilization densities, the $(dT)_{25}$ film consists of randomly coiled ssDNA molecules each anchored via the thiol group and at possibly one or two other bases. We use two examples to demonstrate how the quantitative analysis can be applied to practical problems: the effects of different buffer salts on the immobilization efficiency; the immobilization kinetics. Buffers with divalent salts dramatically increase the efficiency of immobilization and result in very high surface densities ($>5 \times 10^{13}$/ cm^2), densities that may only be possible if the divalent counterions induce strong attractive intermolecular interactions. In contrast with previous reports of alkanethiol adsorption kinetics on gold, ssDNA immobilization in 1 M phosphate buffer does not occur with Langmuir kinetics, a result attributable to rearrangement within the film that follows the initial adsorption.

Introduction

Single-stranded DNA (ssDNA) probes immobilized on solid surfaces are the foundation of a variety of biotechnology applications, ranging from DNA microarrays[1−3] to biosensors.[3−5] Despite the extensive literature describing this bio−surface interface, there are remarkably few publications that directly address the basic mechanisms of ssDNA immobilization or the interactions between individual DNA molecules and surfaces.[5] Practical DNA probes are typically 20−30 bases long,[4] a length range chosen to maximize the efficiency of target hybridization while maintaining specificity. However, even such relatively short sequences contain $\sim 10^3$ atoms and dozens of functional groups, creating multiple intermolecular and probe−surface interactions and therefore making surface analysis challenging. One way to simplify such analysis and obtain precise information about base-specific surface interactions is to use homo-oligonucleotides as model ssDNA.[5] In fact, recent studies of ssDNA-functionalized gold particles[6] and surfaces[7] suggested that there is a significant variation in immobilization and adsorption of the different ssDNA homo-oligonucleotides.

To gain a more comprehensive understanding of ssDNA immobilization, an approach is needed that provides *quantitative* characterization of individual films, while also allowing *direct comparison* between films prepared at different times and under different conditions (with different buffers, for example). Film densities can be measured with standard chemical and biochemical methods such as radiolabeling and fluorescent and electrochemical labeling,[1,4,8] and immobilization can be observed in real time by surface plasmon resonance (SPR).[2,9−11] However, measurements that require labels are not always practical, and their accuracy is dependent on the efficiency of the labeling. Label-free measurements often are subject to ambiguities associated with the detection of nonspecifically immobilized DNA and other chemical changes near the surface. Immobilized

* Address correspondence to this author at Naval Research Laboratory, Code 6177, Washington, DC 20375.
† University of Maryland.
‡ Naval Research Laboratory.
§ National Institute of Standards and Technology.

(1) Pirrung, M. C. *Angew. Chem., Int. Ed.* **2002**, *41*, 1277−1289.
(2) Nelson, B. P.; Grimsrud, T. E.; Liles, M. R.; Goodman, R. M.; Corn, R. M. *Anal. Chem.* **2001**, *73*, 1−7.
(3) Wang, J. *Nucleic Acids Res.* **2000**, *28*, 3011−3016.
(4) Tarlov, M. J.; Steel, A. B. In *Biomolecular Films: Design, Function, and Applications*; Rusling, J. F., Ed.; Marcel Dekker: New York, 2003; Vol. 111.
(5) Kasemo, B. *Surf. Sci.* **2002**, *500*, 656−677.
(6) Storhoff, J. J.; Elghanian, R.; Mirkin, C. A.; Letsinger, R. L. *Langmuir* **2002**, *18*, 6666−6670.
(7) Demers, L. M.; Östblom, M.; Zhang, H.; Jang, N.-H.; Liedberg, B.; Mirkin, C. A. *J. Am. Chem. Soc.* **2002**, *124*, 11248−11249.
(8) Anne, A.; Bouchardon, A.; Moiroux, J. *J. Am. Chem. Soc.* **2003**, *125*, 1112−1113.
(9) Georgiadis, R.; Peterlinz, K. P.; Peterson, A. W. *J. Am. Chem. Soc.* **2000**, *122*, 3166−3173.
(10) Peterlinz, K. A.; Georgiadis, R. M.; Herne, T. M.; Tarlov, M. J. *J. Am. Chem. Soc.* **1997**, *119*, 3401−3402.
(11) Peterson, A. W.; Wolf, L. K.; Georgiadis, R. M. *J. Am. Chem. Soc.* **2002**, *124*, 14601−14607.

10.1021/ja029450c CCC: $25.00 © 2003 American Chemical Society

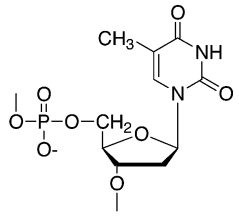

Figure 1. Chemical structure of thymine deoxyribonucleotide (dT). The thymine ring includes two nitrogen atoms in similar bonding configurations that result in a single N 1s XPS core level peak. The two carbonyl groups provide a unique signature in FTIR.

ssDNA films used in biotechnology applications such as DNA microarrays[1−3] are typically <10 nm thick; therefore, standard surface characterization techniques can be employed to complement biochemical analysis.[5,12] Here we describe the use of X-ray photoelectron spectroscopy (XPS) and Fourier transform infrared (FTIR) spectroscopy to characterize the immobilization of ssDNA on gold. These complementary methods provide information about both film coverages and chemical structure within the films and can be used to study samples prepared in the ambient environment without additional in-situ treatment.

In this work we characterize films of thiolated $(dT)_{25}$ probes immobilized on polycrystalline gold surfaces. Thymidine oligonucleotides were chosen because of their relatively simple chemical structure (Figure 1). In addition, the nitrogen atoms and carbonyl groups in the thymine base are associated with specific features in XPS and FTIR spectra, respectively. These features allow us to compare the XPS and FTIR results; we find an almost perfect linear correlation between coverage measurements using the two methods. From analysis of the XPS data we obtain absolute values of the ssDNA coverage that are in good agreement with previous radiolabeling measurements for similar films.[13] Moreover, the coverage dependence of the XPS and FTIR spectra reveals information about the film structure and the interaction of the thymine bases with the gold surface. Finally, we present two examples of how our methods can be applied to practical problems, such as determining the effect of different buffer salts on immobilization and the immobilization kinetics.

Materials and Methods

Materials. We used standard 5′ thiol-modified $(dT)_{25}$ oligonucleotides [3′-$(dT)_{25}(CH_2)_6$SH-5′, from hereon abbreviated $(dT)_{25}$-SH] purchased from Research Genetics. NaCl (Sigma-Aldrich), KCl (J. T. Baker), $MgCl_2 \cdot 6H_2O$ (Mallinckrodt), $CaCl_2 \cdot 2H_2O$ (Sigma-Aldrich), $K_2HPO_4 \cdot 3H_2O$ (Sigma-Aldrich), KH_2PO_4 (Mallinckrodt), and 10 × TE (ResGen, 1 × TE; 10 mM Tris-HCl, 1 mM EDTA) were used to prepare buffer solutions for DNA.[14] Buffers denoted NaCl−TE, KCl−TE, $MgCl_2$−TE, $CaCl_2$−TE, and K_2HPO_4−TE consisted of 1 M solution of respective salt and 1 × TE buffer. The 1 M K_2HPO_4 and KH_2PO_4 buffers without TE were used for measurements of the buffer dependence of the immobilization. All the buffers were adjusted to pH 7 by adding HCl or KOH. A 1 μM DNA solution for immobilization experiments was typically prepared by mixing 25 μL of 200 μM $(dT)_{25}$-SH with 5 mL of buffer. The DNA concentration was confirmed by UV absorption measurements.

Preparation of ssDNA Films. Gold films on single-crystal Si(001) wafers were used as substrates. Prior to the deposition of the films, the wafers were cleaned using a "piranha solution" consisting of 70% H_2SO_4 and 30% H_2O_2 (30% H_2O_2 in H_2O). (*Note that piranha solution must be handled with care: it is extremely oxidizing, reacts violently with organics, and should only be stored in loosely tightened containers to avoid pressure buildup.*) After cleaning, a Cr adhesion layer (20 nm) was deposited by vapor deposition, followed by 200 nm of Au. Each substrate was again cleaned with piranha solution and rinsed thoroughly with deionized water (18.3 MΩ) immediately prior to immobilizing the ssDNA.

$(dT)_{25}$ ssDNA self-assembled monolayers were prepared by immersing clean gold substrates (≈2 cm^2) in 1 μM $(dT)_{25}$-SH solutions (5 mL) at room temperature. We followed the immobilization conditions established in the previous work,[15] which also allowed us to directly compare our results with several quantitative measurements on similar ssDNA films.[9,10,13,15] For time-dependent studies, the immobilization was performed in K_2HPO_4−TE buffer for immersion times of 1, 5, 15, 30, 60, 120, and 1200 min. Immersion for 1200 min in buffers with and without TE was used for studies of the buffer dependence. Before analysis, each sample was rinsed thoroughly with deionized water and blown dry under flowing nitrogen.

FTIR Measurements. FTIR absorption spectra were measured with a Digilab FTS7000 series spectrometer with a PIKE Technologies wire grid infrared polarizer (*p* polarized) and a VeeMax variable angle specular reflectance accessory (reflectance angle 75°).[14] Spectra (2000−800 cm^{-1}) were collected from 1024 scans at 2 cm^{-1} resolution using a cryogenic mercury cadmium telluride detector. The FTIR measurements were performed on freshly prepared samples prior to XPS characterization.

XPS Measurements. XPS spectra were acquired using a commercial XPS system (Thermo VG Scientific Escalab 220i-XL) with a monochromatic Al Kα source and a hemispherical electron energy analyzer.[14] The details of the measurements are described elsewhere.[16] Briefly, normal emission angle-integrated high-resolution scans with 15−20 eV windows and 20 eV pass energy (0.36 eV nominal analyzer energy resolution) were acquired for Au 4f and 4d, O 1s, C 1s, N 1s, and P 2p regions. The S 2p region was also monitored for some of the samples. The reported binding energies were based on the analyzer energy calibration (Au 4f measured at 83.9 eV for all samples); no charge compensation was necessary. Spectra of the N 1s and P 2p regions were accumulated for 30−60 min, depending on the sample coverage, to obtain a good signal-to-noise ratio. As a check on the effects of the incident X-ray beam on the films, a representative sample was exposed for over 3 h, resulting in less than a 5% change in the O, N, and P spectral intensities. Carbon spectra were the most affected by the XPS beam and sample preparation conditions, consistent with the presence of an adventitious hydrocarbon layer. The reference Au signals, used to calibrate the photoelectron attenuation and thickness of DNA overlayers, were measured from Au films cleaned in-situ by Ar ion sputtering.

The peaks in the elemental core-level spectra were fit using commercial XPS analysis software.[17] The number of peaks chosen for each fit was the minimal number required to obtain random residuals. A convolution of Lorentzian and Gaussian line shapes was used to fit the individual peaks, with typical ratios between 10/90 and 20/80. A linear combination of Shirley and linear functions was used to model the background, with the corresponding coefficients fit simultaneously with the peaks. In most cases the full-width at half-maxima (fwhm)

(12) Castner, D. G.; Ratner, B. D. *Surf. Sci.* **2002**, *500*, 28−60.
(13) Steel, A. B.; Levicky, R. L.; Herne, T. M.; Tarlov, M. J. *Biophys. J.* **2000**, *79*, 975−981.
(14) Certain vendors and commercial instruments are identified to adequately specify the experimental procedure. In no case does such identification imply endorsement by the National Institute of Standards and Technology or the Naval Research Laboratory.
(15) Herne, T. M.; Tarlov, M. J. *J. Am. Chem. Soc.* **1997**, *119*, 8916−8920.
(16) Petrovykh, D. Y.; Kimura-Suda, H.; Tarlov, M. J.; Whitman, L. J. Submitted for publication.
(17) Hesse, R.; Chasse, T.; Szargan, R. *Fresenius' J. Anal. Chem.* **1999**, *365*, 48−54.

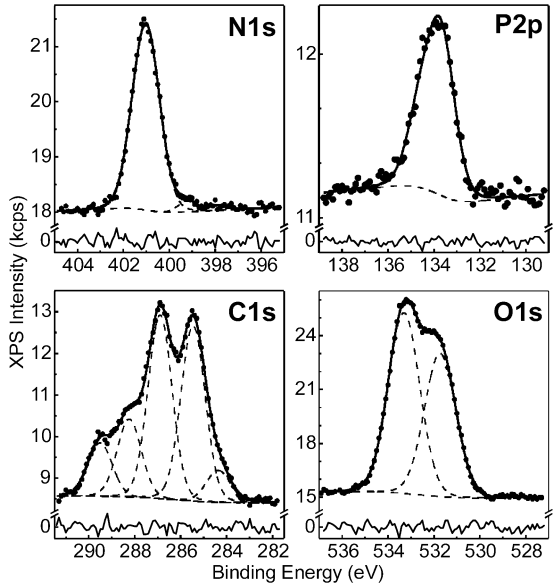

Figure 2. High-resolution XPS spectra for the four principal elements in a DNA film (1 μM $(dT)_{25}$-SH DNA immobilized 1200 min in 1 M K_2HPO_4−TE buffer). A single N 1s peak at 401.0 eV is characteristic of thymine; a single P 2p peak at 133.6 eV is common to all nucleotides. Fitting parameters were chosen for a consistent fit for all samples in the series (filled circles for raw data, thick lines for total fits, and dashed lines for component peaks and background). The minimal number of core level peaks and a combination of Shirley and linear backgrounds were chosen for each of the elements to produce random residuals (thin solid lines below fits).

and background parameters converged to consistent values throughout the series without being restricted, but for a few peaks they were fixed on the basis of values for corresponding spectra with the highest signal-to-noise in the series. The resulting fwhm is the smallest for C 1s peaks (1.3 eV) and the largest for O 1s (1.7 eV)—a range typically observed for polymer-like materials.

Results

XPS Analysis of DNA Films. In Figure 2 we present, to our knowledge, the first published set of high-resolution XPS data for all four principal elements in an immobilized ssDNA film (N, P, C, and O; H is not observable by XPS). Previous measurements for related systems include two ∼30-year-old datasets for adsorbed DNA bases[18,19] and, more recently, limited results for thymine[20] and DNA films.[15,21,22] In contrast to prior work, our spectra were obtained with a high-intensity, monochromatized Al Kα X-ray source that enables superior energy resolution and excellent signal-to-noise, attributes that allow us to observe the detailed evolution of the N 1s spectra with immobilization time, as shown in Figure 3.

The principal N 1s core level peak has a binding energy between 400.5 and 401.0 eV, consistent with published results for thymine multilayers (401.1−402.1[18] and 400.4 eV[20]) and powder (400.9 eV[19]). Because very similar chemical shifts are expected for both N atoms in each thymine ring (Figure 1),[23−25]

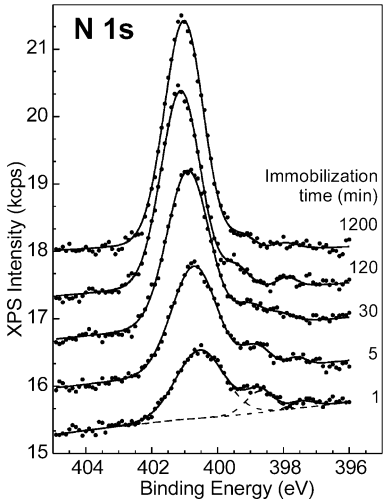

Figure 3. Evolution of the N 1s XPS peak with increasing immobilization time for 1 μM $(dT)_{25}$-SH in 1 M K_2HPO_4−TE buffer. The monotonic peak shift with increasing film thickness, up to ≈0.5 eV, is characteristic of extraatomic relaxation in organic films. The satellite peaks shifted by about −1.8 and −3.1 eV are attributed to chemisorbed thymine rings observed primarily at low coverages.

we fit the series shown in Figure 3 using a single main N 1s peak with 1.5−1.6 eV fwhm (10/90 Lorentian/Gaussian convolution). A shift to higher binding energy with increasing DNA coverage is apparent in the spectra. The shift monotonically increases for the first three samples, saturating at about 0.5 eV for the thickest films in this series. Such shifts are common in organic multilayers on metal surfaces and are typically attributed to extraatomic relaxation and charging effects.[26] We observe similar shifts for the other elements.

In addition to the bulk-thymine-like N 1s peak, lower binding energy components are observed that are shifted by approximately −1.8 and −3.1 eV (Figure 3). They are most prominent for the lowest coverage, and both the relative and absolute intensities of these features decrease with increasing coverage. A chemical shift to lower binding energy of this magnitude in organic multilayers has been attributed to bond formation between the molecules and the substrate, i.e., chemisorption.[26] In fact, the peak shifted 1.8 eV is consistent with the 1.5 ± 0.2 eV shift reported for thymine chemisorbed on Au(111) in an upright position,[20] and 3.1 eV is comparable to the shift reported for chemisorption of acetonitrile on Pt(111) in a flat geometry.[26] In control experiments (not shown), we observed that nonspecific adsorption on gold of $(dT)_{25}$ probes without a thiol produced multiple N 1s peaks within 4−5 eV from the bulk-thymine value.

The presence of N[15,22] or, to a better extent, N and P together, is an excellent indicator of adsorbed DNA[21] because their presence is typically unaffected by surface contamination during sample preparation and handling. Thymidine nucleotides (Figure 1) contain more N atoms than P, and N has a higher XPS cross section; so between the two, N provides a more reliable reference for composition measurements. Hence the ratios of the other elements to N can be compared to those expected for the nucleotide under study as a measure of film quality. The

(18) Barber, M.; Clark, D. T. *Chem. Commun.* **1970**, 24−25.
(19) Peeling, J.; Hruska, F. E.; McIntyre, N. S. *Can. J. Chem.* **1978**, *56*, 1555−1561.
(20) Roelfs, B.; Bunge, E.; Schroter, C.; Solomun, T.; Meyer, H.; Nichols, R. J.; Baumgartel, H. *J. Phys. Chem. B* **1997**, *101*, 754−765.
(21) Zhao, Y. D.; Pang, D. W.; Hu, S.; Wang, Z. L.; Cheng, J. K.; Qi, Y. P.; Dai, H. P.; Mao, B. W.; Tian, Z. Q.; Luo, J.; Lin, Z. H. *Anal. Chim. Acta* **1999**, *388*, 93−101.
(22) Wang, J.; Rivas, G.; Jiang, M. A.; Zhang, X. J. *Langmuir* **1999**, *15*, 6541−6545.
(23) Mely, B.; Pullman, A. *Theor. Chim. Acta* **1969**, *13*, 278−287.
(24) Snyder, L. C.; Shulman, R. G.; Neumann, D. B. *J. Chem. Phys.* **1970**, *53*, 256−267.
(25) Rein, R.; Nir, S.; Hartman, A. *Isr. J. Chem.* **1972**, *10*, 93−100.
(26) Sexton, B. A.; Hughes, A. E. *Surf. Sci.* **1984**, *140*, 227−248.

base-specific P/N ratio is particularly useful—1/2 for dT, 1/3 for dC, and 1/5 for dA and dG—because N and P are contained exclusively in the bases and the backbone, respectively. Their presence in the proper stoichiometric ratio is an indication that a film has not degraded before or during characterization.

An additional factor that might interfere with elemental characterization is the presence of residual contaminants from the buffer solution. We find that the P/N ratio does not increase when phosphate rather than chloride buffers are used, indicating that phosphate salts do not contaminate the P signal. Some buffers do leave trace contaminants. For K_2HPO_4, from 0.3 to 3 at. % of K is observed with increasing immobilization time. A submonolayer of iodine is also detected on some samples, with the amount increasing with immobilization time, most likely arising from trace amounts of iodide in the buffers.

For thiolated probes, the sulfur signal is also of interest. However, the S core levels are intrinsically difficult to observe for $(dT)_{25}$-SH samples because of the very low relative concentration of sulfur atoms (the ideal S/P ratio is 1/25) and the strong attenuation of the signal by the overlaying DNA.[16] The typical signal-to-noise ratio for the S *2*p peaks is only 2 or 3 for practical acquisition times, causing an uncertainty of the S *2*p signal intensity of about 50%. We find that the typical S 2p/Au 4f intensity ratios for our $(dT)_{25}$-SH films are 1 order of magnitude lower than those reported for alkanethiol self-assembled monolayers,[27] consistent with the relatively lower packing density expected for the ssDNA films. For all $(dT)_{25}$-SH samples where signal intensity was sufficient for fitting, the S $2p_{3/2}$ peak binding energy was 162.0 eV, consistent with a thiolate S—Au bond.[28−31] We do not observe any features in the 163−164 eV binding energy range, associated with unbound thiol groups,[28−32] which we interpret as evidence that there was very little physisorbed ssDNA in the films under investigation.

FTIR Results. FTIR spectra are shown in Figure 4 for the actual samples characterized by XPS in Figures 2 and 3. The prominent absorbance peak at 1714 cm^{-1} is specific to the carbonyl groups in the thymine ring (Figure 1). The position of this peak is consistent with a previous in-situ IR study of thymine adsorption on Au(111) that assigned the carbonyl stretching feature to free thymine in solution (i.e., not adsorbed on the surface).[33] We therefore attribute the 1714 cm^{-1} feature in our study to thymine bases that are contained in the DNA monolayer but are not interacting strongly with the gold surface (from hereon denoted "nonchemisorbed"). We observe that the position of the main carbonyl peak shifts slightly depending on the valence of the buffer cations: the peak is at ≈1714 cm^{-1} for monovalent cations and at ≈1718 cm^{-1} for divalent cations.

The FTIR spectra also provide corroborating evidence for strong thymine−substrate interactions at lower DNA coverages.

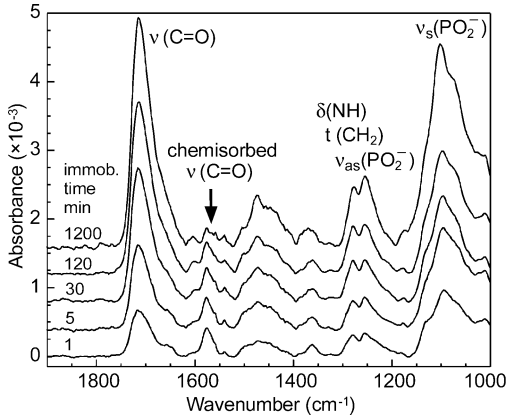

Figure 4. Evolution of FTIR spectra with increasing immobilization time for 1 μM $(dT)_{25}$-SH in 1 M K_2HPO_4−TE buffer. The peak at 1714 cm^{-1} corresponds to carbonyl groups in free thymine rings (and is specific to dT nucleotides). Peaks between 1550 and 1600 cm^{-1} are attributed to chemisorbed thymine.

The spectra are rich with features associated with various functional groups, so identification and quantification of peaks specific to carbonyl groups in chemisorbed thymine rings is difficult. Nonetheless, a feature is observed between 1550 and 1600 cm^{-1} that clearly *decreases* with increasing coverage (Figure 4). This frequency range is consistent with that previously reported for carbonyl modes in thymine chemisorbed on Au(111).[33] In this earlier study, Hais et al. interpreted two carbonyl features in this range to originate from thymine chemisorbed to Au through the N3 nitrogen. Because the immobilization time dependence of the 1550−1600 cm^{-1} carbonyl features is qualitatively similar to that observed in Figure 3 for the N 1s satellite peaks, we interpret these modes to be the FTIR signature of the chemisorbed bases.

Discussion

Correlation between XPS and FTIR Results. (a) Coverage Determination. The XPS and FTIR spectra provide independent, complementary measurements of the relative coverages. The XPS results can also be used to calibrate the coverages absolutely. For the FTIR data, we use the nonchemisorbed carbonyl absorbance peak for the coverage determination. The absolute values of the absorbance are small for this peak, even for the thickest DNA film; therefore, the attenuation is negligibly small and the absorbance is simply proportional to the amount of thymine. We use the peak area integrated between 1615 and 1800 cm^{-1} to find the $(dT)_{25}$-SH DNA coverage from the FTIR data, represented by the solid triangles in Figure 5. Although orientation effects could possibly affect the linearity of the dependence of peak area on coverage, given the short persistence length of ssDNA, the films are likely to be disordered. Indeed, in considering FTIR and XPS data below, carbonyl peak areas do not seem to be significantly influenced by orientation effects of $(dT)_{25}$-SH probes.

The absolute intensity of an XPS core level peak depends on the thickness of the film. However, this effect can be *quantitatively* taken into account using an overlayer model. In the model, the observed intensity of the Au substrate signal I_{Au} is given by the intensity from a clean Au substrate I^0_{Au} attenuated by the DNA film of thickness t (eq 1). Likewise, the observed intensity I_X from element X in the overlayer is the intensity from a half-infinite slab of the same material I^∞_X

(27) Kawasaki, M.; Sato, T.; Tanaka, T.; Takao, K. *Langmuir* **2000**, *16*, 1719−1728.
(28) Castner, D. G.; Hinds, K.; Grainger, D. W. *Langmuir* **1996**, *12*, 5083−5086.
(29) Bensebaa, F.; Yu, Z.; Deslandes, Y.; Kruus, E.; Ellis, T. H. *Surf. Sci.* **1998**, *405*, L472−L476.
(30) Laibinis, P. E.; Whitesides, G. M.; Allara, D. L.; Tao, Y. T.; Parikh, A. N.; Nuzzo, R. G. *J. Am. Chem. Soc.* **1991**, *113*, 7152−7167.
(31) Rieley, H.; Kendall, G. K.; Zemicael, F. W.; Smith, T. L.; Yang, S. H. *Langmuir* **1998**, *14*, 5147−5153.
(32) Buckel, F.; Effenberger, F.; Yan, C.; Golzhauser, A.; Grunze, M. *Adv. Mater.* **2000**, *12*, 901−905.
(33) Haiss, W.; Roelfs, B.; Port, S. N.; Bunge, E.; Baumgartel, H.; Nichols, R. J. *J. Electroanal. Chem.* **1998**, *454*, 107−113.

reduced to account for the finite layer thickness t (eq 2).

$$I_{Au} = I^{0}_{Au} \exp(-t/L_{Au}) \quad (1)$$

$$I_X = I^{\infty}_X(1 - \exp(-t/L_X)) \quad (2)$$

Fortunately, the model can be reduced to a combination of well-known and directly measured parameters, allowing quantitative calibration with a high degree of confidence.[12,34] The detailed description of the XPS data analysis is presented elsewhere[16] but can be summarized as follows:

The effective attenuation length (EAL) in the DNA film for electrons from gold (L_{Au}) and the DNA elements (L_X) is calculated using the NIST Standard Reference Database[35,36] software. We use the absolute intensity reference for Au in this work, whereby film thickness t is determined using eq 1 from Au $4f_{7/2}$ and $4d_{5/2}$ peak intensities measured for a clean Au substrate and for DNA/Au samples. To interpret the measured intensity ratio I_X/I_{Au}, the prefactors I^0_{Au} and I^{∞}_X in eqs 1 and 2 can be expanded as products of respective experimental parameters, and their ratio can be reduced to a constant[37] multiplied by N_X—the atomic density of the element X in the film (relative to Au density). Using data for nitrogen as a DNA-specific element, the product of N_N and film thickness t is proportional to DNA coverage (the open circles Figure 5). Assuming the proper nucleotide stoichiometry, the absolute value of the coverage in molecules/cm^2 can be calculated with an uncertainty estimated to be <20%.[16] We find that after immobilizing the $(dT)_{25}$-SH ssDNA for 1200 min, the absolute coverage is 3.7×10^{13} molecules/cm^2 (Figure 5, right axis). This coverage is in good agreement with that determined by radiolabeling a thiolated 24-base-long probe immobilized under the same conditions.[13]

When comparing coverages determined by FTIR versus XPS (Figure 5), it is important to note that the FTIR coverage was determined from the peak associated with nonchemisorbed bases (because the features associated with chemisorbed bases are not easily deconvolved from other peaks). In contrast, the XPS coverage was determined by integrating all spectral features, including those from chemisorbed bases, so this coverage is always slightly higher. The diminishing difference between the two values with increasing coverage is one of the indications that the film ultimately becomes dominated by free-standing molecules.

If we compare only the coverages associated with nonchemisorbed bases (integrating only the main N 1s peak) and normalize the FTIR and XPS coverages to their respective maxima, there is a nearly perfect linear correlation between the two measurements (solid circles and line in Figure 6). This correlation is important given the completely different physics of the two measurements, providing strong support for the validity of the models used to convert the spectra into coverages.

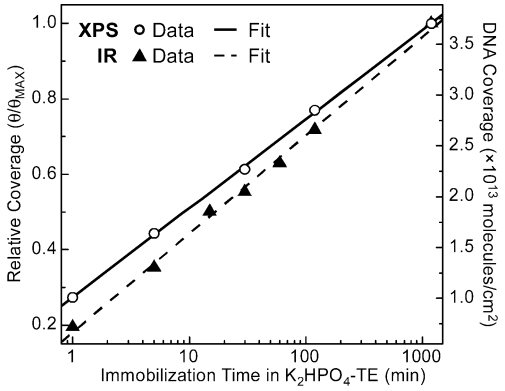

Figure 5. $(dT)_{25}$-SH DNA coverage as a function of immobilization time in a 1 M K_2HPO_4−TE buffer. Open circles are from XPS data that include both nonchemisorbed and chemisorbed thymine components. Solid triangles are from FTIR data for nonchemisorbed molecules only, and so the values are lower than for XPS, particularly at low coverages. The relative coverage (left axis) is normalized to the respective maxima. The absolute coverage (right axis) is calibrated from quantitative analysis of the XPS data.

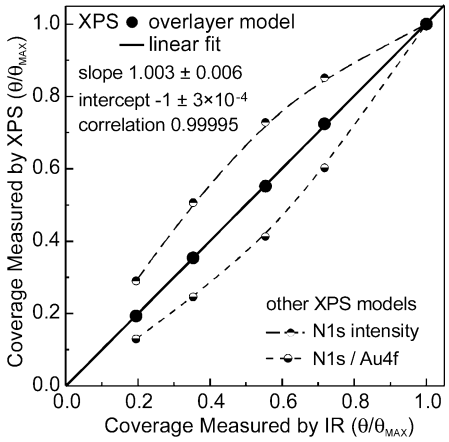

Figure 6. $(dT)_{25}$-SH DNA coverage calculated from XPS and IR data and normalized to the respective maxima. In both cases only the signals associated with nonchemisorbed thymine are considered (the N 1s peak at 401 eV and C═O peak at 1714 cm^{-1}, respectively). When the XPS coverage is analyzed, using an overlayer model to account for electron attenuation, there is a nearly perfect correlation between the coverages obtained for the two techniques. In contrast, the raw N 1s intensity underestimates the coverages and a simple N 1s/Au 4f ratio overestimates them.

For example, whereas FTIR is sensitive to the orientation of carbonyl groups, XPS is not, and so the excellent correlation indicates that the average orientation of the bases does not change with coverage. Although, as we discuss below, the configuration of the individual ssDNA molecules (and their lateral ordering) changes with increasing coverage, the local orientation of the individual bases apparently remains random.

The importance of correctly accounting for attenuation effects in the XPS analysis is demonstrated by comparing the results with those from two simpler methods often used to estimate coverage from XPS spectra. The first method, using only the relative intensity of the N 1s peak, underestimates the amount of adsorbed DNA for the highest coverage samples because the films are thick enough to attenuate the signal from N atoms closest to the substrate. Therefore, this measure of the coverage leads to apparent saturation near maximum coverage and inflates the relative value for low coverages (top half-filled circles and dashed line in Figure 6). The second method, using the N 1s peak normalized to the substrate Au $4f_{7/2}$ peak, overestimates the coverage because the gold signal is attenuated stronger with

(34) Ratner, B. D.; Castner, D. G. In *Surface Analysis-The Principal Techniques*; Vickerman, J. C., Ed.; Wiley: Chichester, U.K., 1997; pp 43−98.
(35) Powell, C. J.; Jablonski, A. *NIST Electron Effective-Attenuation-Length Database Version 1.0*; NIST: Gaithersburg, MD, 2001.
(36) Jablonski, A.; Powell, C. J. *Surf. Sci. Rep.* **2002**, *47*, 35−91.
(37) Parameters determined by the experimental configuration (X-ray flux, illuminated sample area, analyzer acceptance) cancel out in the ratio. Instrumental transmission function values are provided by the manufacturer and can be independently checked, e.g. by measurements of multiple Au peaks on clean Au samples. Scofield sensitivity factors for the respective atomic orbitals are tabulated. EAL's and emission anisotropy factors are calculated using the NIST SRD software.[35,36] See ref 16 for details.

increasing coverage (bottom half-filled circles and short-dashed line in Figure 6).

Because each nucleotide contains all four principal elements within DNA, elemental densities N_X calculated from the overlayer model can be used to evaluate the stoichiometry of the film. (As discussed above, raw peak intensities would give incorrect elemental ratios.) In the $(dT)_{25}$-SH immobilization series, the average P/N ratio is 0.58, in good agreement with 0.5 expected for a stoichiometric dT nucleotide (Figure 1). The C/N ratio decreases from 8.3 to 5.8 with increasing DNA coverage. The theoretical value is 5 in this case, and so the data indicate that hydrocarbon contamination is least significant on the highest coverage films. The O/N ratio decreases from 4.3 to 3.8, a ratio close to the stoichiometric value of 3.5, indicating that very little water is trapped in the films.

(b) Film Structure. We have established that both the FTIR and XPS spectra are dominated by signatures of nonchemisorbed bases in the DNA film and that the relative and absolute density of bases strongly chemisorbed on the substrate decreases as the coverage increases. In terms of the film structure, this decrease implies that the bulk of the $(dT)_{25}$-SH ssDNA in the film is not in contact with the substrate. Given the strongly attenuated XPS sulfur signal, with binding energy characteristic of thiolate bonding, the results indicate that at high coverage the ssDNA molecules form a free-standing, self-assembled monolayer anchored via the thiol groups.

On the basis of the low-coverage data, we can estimate that initially about a third of the bases are chemisorbed. If we assume a uniform distribution of the chemisorbed bases, then at the lowest coverage each dT-25mer has about eight bases in contact with the substrate. From the residual XPS and FTIR chemisorbed component intensities, only about one or two bases per strand are chemisorbed at the highest coverage. Therefore, we conclude that the $(dT)_{25}$-SH film structure changes from ssDNA molecules lying nearly flat on the substrate, anchored in multiple locations, to randomly coiled ssDNA molecules anchored via a thiol group and at, possibly, one or two other bases. As discussed above, the correlation between the XPS and FTIR coverages suggests that there is no preferred orientation of the bases versus coverage in this series.

Buffer and Immobilization Efficiency. It is generally known that varying the ionic strength or identity of salts used in buffer solutions affects the immobilization efficiency of polyelectrolytes.[38] We expect the immobilization of DNA to be similarly affected. In the simplest model, changing the cation can increase the screening between charged ssDNA strands, decreasing the repulsive interaction, and thereby result in a higher density of immobilized probes (or, conversely, can decrease the screening and lower the density). The coverage as measured by FTIR and XPS after 1200 min of immobilization in a number of different buffers is presented in Figure 7 (all for 1 μM $(dT)_{25}$-SH in 1 M salt with TE, except where indicated otherwise). For the four monovalent cation buffer salts, we again find good agreement between the relative coverage determined by the two techniques, allowing us to calibrate the absolute coverage based on the XPS data. For the two divalent buffers, the coverage from the FTIR spectra is notably higher than that from XPS, the reasons for which will be discussed below.

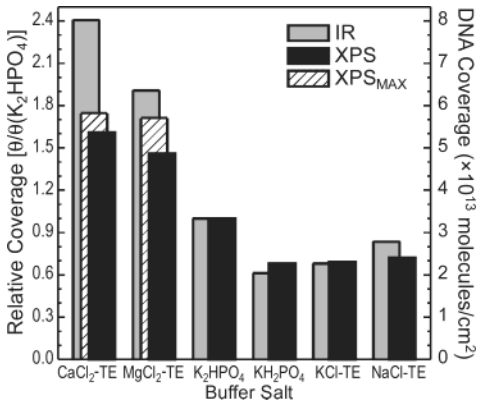

Figure 7. Effect of buffer salt on immobilization efficiency, as indicated by the DNA coverage after 1200 min in solutions of 1 μM $(dT)_{25}$-SH in various buffers. The gray (FTIR) and black (XPS) bars are the coverages for 1 M buffers. The relative coverages (left axis) are normalized to that of the K_2HPO_4 sample (compare to 1200 min in K_2HPO_4−TE, Figure 5). The absolute coverages (right axis) are calibrated from the XPS data. Hatched bars are for surfaces with the observed maximum coverage (by XPS), obtained with 2 M $CaCl_2$ and 0.1 M $MgCl_2$.

The coverage obtained with K_2HPO_4 buffer alone is about 10% lower than with TE (see Figure 5), but the difference is comparable to scatter within individual datasets. Therefore, the addition of TE to phosphate buffers does not appear to significantly affect the immobilization density. Buffers with Na and K monovalent cations show similar immobilization efficiency, independent of the anion. Doubling the monovalent cation concentration by using K_2HPO_4 instead of KH_2PO_4 increases the coverage by about 50%. A similar coverage increase was observed for NaCl−TE in a control experiment with 2 M vs 1 M concentration (not shown). The cation valence has a larger effect on immobilization than its concentration—by either XPS or FTIR the coverage increases more than 100% when divalent cation buffers are used. Interestingly, the way that the coverage depends on salt concentration is distinctly different between the two divalent cations, Ca^{2+} and Mg^{2+}. Increasing the Ca^{2+} concentration from 0.01 to 2 M results in a monotonic coverage increase followed by a drop off at 3 M (the change from 0.01 to 2 M is qualitatively similar to the effect of Na^{1+}). In contrast, with Mg^{2+} the coverage peaks at 0.1 M.

Surprisingly, the coverage obtained with the two divalent buffers corresponds to an average spacing between the individual ssDNA probes of ~1 nm, a distance comparable to the radius of a DNA double helix. To achieve such a packing density with single-stranded homo-oligonucleotides, i.e., without base-pairing, would require some type of cross-linking or aggregation. We speculate that divalent cations may cause intermolecular or intramolecular electrostatic cross-linking of the negatively charged ssDNA, leading to more compact molecular conformations at the surface. Two possible scenarios include ssDNA aggregation in solution prior to immobilization and base stacking between the nearest-neighbor immobilized probes. An attractive interaction between closely spaced negatively charged polyelectrolyte molecules is predicted for divalent buffers on the basis of counterion condensation theory and its extensions[39] and applied to ssDNA would predict cross-linking of the charged backbones.

(38) Zhang, Y. Y.; Tirrell, M.; Mays, J. W. *Macromolecules* **1996**, *29*, 7299−7301.

(39) Anderson, C. F.; Record, M. T. *Annu. Rev. Phys. Chem.* **1982**, *33*, 191−222.

One indication that intermolecular base stacking may be occurring comes from the anomalously large FTIR signals observed with the 1 M divalent buffers (Figure 7). The "coverages" determined from the carbonyl stretch are notably higher than even the maximum observed by XPS (with 2 M $CaCl_2$ and 0.1 M $MgCl_2$). A relative increase in the intensity of the carbonyl stretch/molecule would imply that these bases are preferentially oriented, with the plane of the rings perpendicular to the surface. The FTIR signal enhancement is larger with Ca^{2+} cations, indicating that the film ordering is affected by the identity of the cations as well as their valence. In addition, our preliminary results for other oligonucleotides indicate that the anion used may also affect interactions between the bases. The results of our more extensive study of these effects will be discussed in future publications.

Immobilization Kinetics. It is generally believed that thiolated ssDNA probes adsorb on gold with Langmuir kinetics,[4] similar to that observed for alkanethiols.[40] In fact, modified second-order Langmuir kinetics have been reported in an SPR study[9] of adsorption of a thiolated 24-base ssDNA probe under the same conditions used in our work. However, the immobilization we observe, shown in Figure 5, definitely does *not* have a Langmuir time dependence. First- or second-order Langmuir kinetics would appear as a sigmoidal curve on this semilog plot, whereas the observed kinetics are essentially linear in log time.[41] This discrepancy cannot be attributed solely to the different measurement techniques. For the classic case of alkanethiol adsorption on gold, the coverage measured by XPS has been consistent with Langmuir-like kinetics.[27] For example, Figure 11 in ref 27 shows the time dependence in essentially the same coordinates as those in our Figure 5, and the adsorption curves are distinctly nonlinear in that case. It is clear that SPR and XPS give consistent results for alkanethiol adsorption but not for thiolated ssDNA.

The most likely source of the systematic discrepancy between the SPR and XPS results for ssDNA is the difference between the in-situ SPR and ex-situ XPS measurement. SPR is not sensitive specifically to DNA but to the presence of an adsorbed layer, in general, so the coverage measured by SPR (or by other in-situ methods, e.g. quartz crystal microbalance or UV absorption) will include contributions from all near-surface species. In fact, up to 60% loss of ssDNA after rinsing is observed by SPR,[11] which we interpret as removal of nonspecifically adsorbed molecules. XPS, on the other hand, is carried on rinsed samples and is specifically sensitive to N and P from DNA. We thus believe that, even though XPS is performed ex situ, the elemental specificity of the technique provides a fundamentally more reliable measurement of *immobilized* DNA coverage.

The linear in log time immobilization kinetics we observe is very unusual. One common cause for non-Langmuir kinetics is diffusion-limited adsorption, but that case produces a square root of time dependence. A more likely explanation of our results comes from modeling studies: a linear in log time kinetics is predicted for a polyelectrolyte adsorption under high salt conditions, where molecular reorganization on the surface becomes a rate-limiting step.[42] This interpretation is consistent with the time dependence of the chemisorbed components we observe that suggests rearrangement from ssDNA initially lying nearly flat on the substrate to a final anchored random coil configuration at high coverage.

Summary and Conclusions

We demonstrate the use of XPS and FTIR surface analysis to characterize the immobilization of ssDNA on gold. Thiolated $(dT)_{25}$ ssDNA is used as a model system that provides specific and complementary spectral signatures for the two characterization methods and enables us to extract quantitative information about the coverage and DNA−substrate interactions. XPS analysis provides a coverage determination calibrated against the bulk density of the gold substrate, enabling absolute coverages to be quantitatively compared between samples prepared under widely varying conditions. We find maximum coverages (depending upon the buffer) in the range of $(1-6) \times 10^{13}$ molecules/cm^2. We also demonstrate that an excellent correlation between FTIR and XPS coverage measurements can be obtained when the data are carefully analyzed. On the basis of the evolution of the spectral features during immobilization, we conclude that the $(dT)_{25}$-SH film structure changes initially from ssDNA molecules lying nearly flat on the substrate, anchored in multiple locations, to randomly coiled ssDNA molecules anchored via the thiol group and at possibly one or two other bases.

We observe strong effects of different buffer salts on the immobilization efficiency and find surprising immobilization kinetics in a standard phosphate buffer, results with potentially immediate practical impact. Using a divalent versus monovalent cation has a much larger effect on immobilization than simply doubling the concentration of the monovalent cation. In the phosphate buffer the immobilization kinetics shows a linear in log time behavior, very different from the Langmuir-like kinetics reported for similar systems characterized with other techniques. The unusual functional form of the kinetics suggests that the $(dT)_{25}$-SH ssDNA immobilization is more complicated than that for alkanethiol SAM formation, probably involving substantial rearrangement of the molecular film following the initial adsorption.

We have shown that XPS and FTIR can be used for the quantitative analysis of the coverage, structure, and chemistry of DNA films. The wide availability of FTIR and XPS instruments suggests that this methodology can be incorporated as part of routine characterization of DNA-functionalized surfaces.[5,12] In particular, the use of XPS for coverage determination is generally applicable, because it involves a minimal set of assumptions that are typically satisfied for biological films. In contrast, FTIR *needs to be properly validated and calibrated* (e.g. vs XPS measurements) before it can be used for coverage measurements, because FTIR peak intensities strongly depend on the orientation of the molecules in the film (which is typically not known a priori). Correspondingly, a nonlinear correlation between FTIR and XPS results can be considered evidence of preferential molecular orientation in the film. Preliminary experiments with the other three homo-oligonucleotides [oligo(dA), oligo(dC), and oligo(dG)] indicate that characteristic

(40) Schwartz, D. K. *Annu. Rev. Phys. Chem.* **2001**, *52*, 107−137.
(41) For practical reasons, this experiment has not been continued long enough to achieve an apparent saturation of the coverage. In experiments using the 1 M NaCl−TE buffer, the coverage showed a similar linear increase between 1 and 1200 min and saturated after 8400 min at a lower value consistent with the buffer dependence in Figure 7.
(42) Cohen Stuart, M. A.; Hoogendam, C. W.; de Keizer, A. *J. Phys.*: *Condens. Matter* **1997**, *9*, 7767−7783.

FTIR spectral features can be used to reliably identify nucleotides present on a surface, a task that is less definitive using only XPS spectra (especially for mixtures). In addition, it may be possible to use spectral features to specifically identify DNA duplex formation. We are also exploring the possibility of extending the DNA coverage determination by XPS to more practical films, such as those containing diluent thiols or biocompatible polymers, which should be straightforward as long as the N or P content of the film is exclusive to DNA. Finally, we hope that our novel observations for model DNA systems together with high-resolution spectra and quantitative analysis will stimulate further theoretical study of the adsorption and structure of immobilized DNA films.

Acknowledgment. D.Y.P. and L.J.W. are grateful for stimulating discussions about DNA immobilization with Drs. Paul Sheehan and Thomas Clark (NRL) and Professor George Schatz (Northwestern University). M.J.T. thanks Professor Rastislav Levicky (Columbia University) for initiating the FT-IR studies of DNA on gold while a NIST-NRC Postdoctoral Associate. H.K.-S. thanks Dr. Peter Vallone (NIST) for his assistance characterizing the DNA samples and Dr. Tina Huang (NIST) for advice on DNA immobilization. Work at NRL was supported by the Office of Naval Research and the Air Force Office of Scientific Research.

JA029450C